Catalysis Today 454 (2025) 115288

Contents lists available at ScienceDirect

Catalysis Today

journal homepage: www.elsevier.com/locate/cattod

Catalytic behavior of ITQ-13 zeolite in benzene and toluene ethylation

M. Teresa Portilla [a,c], Avelino Corma [a], Cristina Martínez [a], Susana Valencia [a], Francisco J. Llopis [b,*]

[a] Instituto de Tecnología Química (UPV-CSIC), Universitat Politècnica de València - Consejo Superior de Investigaciones Científicas, Av. De los Naranjos s/n, 46022 Valencia, Spain
[b] Departamento de Ingeniería Química, UV, Universitat de València, Avd Universidad, s/n, Burjassot, Valencia 46100, Spain
[c] currently working on: R&D Department of International Flavors & Fragrances (IFF), Av. Felipe Klein 2, Benicarló 12580, Spain

ARTICLE INFO

Keywords:
ITQ-13 zeolite
Alkylation
Benzene
Toluene

ABSTRACT

The ITQ-13 zeolite (ITH) presents a three-dimensional channel system formed by channels delimited by rings of 9 and 10 tetrahedra (9MR and 10MR). This material has been studied as a catalyst in reactions of interest in the petrochemical industry, which are carried out on a commercial scale in the presence of medium-pore zeolites, such as the alkylation of benzene or toluene with ethylene or ethanol. Due to its acidic properties and its particular topology, zeolite ITQ-13 presents a comparable activity to that of ZSM-5 or MCM-22, employed at commercial scale, but also higher selectivity to the main alkylation products and lower deactivation rate. The large cavities located at the intersections between the 9MR and 10MR channels, capable of hosting larger reaction intermediates than ZSM-5, and the greater activity of its external surface, could be responsible for the improved catalytic behavior of ITQ-13.

1. Introduction

The alkylation of aromatic compounds with ethanol can be effectively accomplished through heterogeneous catalytic processes, with zeolites playing a pivotal role. Zeolites are microporous aluminosilicates characterized by a high surface area and exceptional catalytic properties, making them ideal candidates for facilitating a wide range of chemical reactions. Their crystalline frameworks consist of interconnected channels and cavities, whose size and geometry govern the behavior of reactants, products, and transition states. This structural feature, referred to as shape selectivity, directly influences the selectivity of the process [1,2].

Zeolite ITQ-13 (ITH) exhibits a three-dimensional multipore structure with interconnected 9 and 10 membered ring (MR) channels [3]. Although it, bears some structural similarities to that of ZSM-5 (MFI), it presents a more complex channel system, with 9-membered ring (9MR) pore aligned with the *a*-axis and possessing dimensions of approximately 4.0 × 4.9 Å, analogous to those of the 10MR channels of MCM-22 (MWW). The 10MR channels oriented along the *b*- and *c*-axes, with apertures of approximately 4.8 × 5.1 Å and 4.8 × 5.3 Å, respectively, are more similar to those of ZSM-5. These 9MR and 10MR channels are interconnected by a large cylindrical cavity, 4.8 × 5.3 Å (cross section) and 15.5 Å (length) capped by double four ring units (D4R) at both ends [4]. Notably, zeolites with 9MR channels are rare, making ITQ-13 a potentially interesting candidate for catalyzing aromatic alkylation reactions, industrially performed using ZSM-5 or MCM-22.

Alkylated aromatics, such as ethylbenzene and ethyltoluene, are critical intermediates in the production of a wide array of chemicals, including polystyrene and polymethylstyrene resins. Traditionally, the synthesis of these compounds has been heavily reliant on petrochemical feedstocks, which are associated with significant greenhouse gas emissions and resource depletion. The use of zeolites in the alkylation of aromatic compounds with ethanol offers several advantages in terms of sustainability. Zeolites enhance reaction efficiency, leading to higher yields of alkylated aromatics while minimizing by-products and waste [5]. This contributes to Sustainable Development Goal (SDG) 12 (Responsible Consumption and Production) by promoting efficient resource utilization and waste reduction. Additionally, zeolites are recyclable, retaining high catalytic activity over multiple cycles, which supports the principles of a circular economy [6].

Ethanol, derived from renewable biomass such as sugarcane and corn, provides a sustainable alternative to fossil fuel-based feedstocks. Its incorporation into alkylation processes aligns with SDG 7 (Affordable and Clean Energy) by promoting the use of bio-based chemicals and

* Corresponding author.
E-mail address: francisco.llopis@uv.es (F.J. Llopis).

https://doi.org/10.1016/j.cattod.2025.115288
Received 15 January 2025; Received in revised form 27 February 2025; Accepted 19 March 2025
Available online 22 March 2025

reducing dependence on non-renewable resources.

In the present study, ITQ-13 zeolite has been investigated as a catalyst for the alkylation of benzene and toluene with ethanol, reactions of significant interest in petrochemical processes. These alkylation reactions are typically conducted using medium-pore zeolites [7, 8]. The catalytic performance of ITQ-13 is compared to that of the widely used zeolites ZSM-5 and MCM-22, which are commonly employed in commercial-scale processes.

2. Experimental

2.1. Synthesis of zeolites

The ITQ-13 zeolite was synthesized using the procedure described by Corma et al. [4,9]. The structure-directing agent used was hexamethonium dihydroxide ($R(OH)_2$) and the molar composition of the synthesis gel was 0.91 SiO_2: 0.09 GeO_2: 0.01 Al_2O_3: 0.25 $R(OH)_2$: 0.5 HF: 5 H_2O. The synthesis mixture was prepared by adding the required amount of GeO_2 Aldrich) in an aqueous solution of hexamethonium dihydroxide (0.1 M, Aldrich), followed by the addition of tetraethylorthosilicate (TEOS) (98 %, Merck). The resulting solution was stirred until the complete hydrolysis of TEOS was achieved and the ethanol generated was evaporated. Then, 10 wt% of seeds (with respect to the inorganic oxides) of ITQ-13 zeolite (Si/Ge = 20), prepared according to [9], were added and, finally, the appropriate amount of hydrofluoric acid (48 % aqueous solution, Aldrich) was incorporated. It is worth mentioning that the use of hydrofluoric acid must be carried out with appropriate safety protections, such as the use of adequate gloves and handling inside a fume hood among others, in particular the protocol of the UPV Prevention Service was followed [10].

The final synthesis mixture was introduced in Teflon-lined stainless steel autoclaves and the crystallization was carried out in an oven at 448 K under rotation (60 rpm) for 3 days. The obtained product was filtered, washed with deionized water, and subsequently dried overnight at 373 K. The hexamethonium cations occluded in the structure were removed by calcination of the zeolite at 853 K for 3 hours and the acid form was thus obtained.

The zeolitic material MCM-22, with a Si/Al ratio of 50, was synthesized following the method described by Leonowicz et al. [11], using hexamethyleneimine as the organic structure-directing agent (SDA). The zeolite was converted to its acid form by calcination at 853 K, followed by ion exchange with an aqueous solution of NH_4Cl at 353 K to exchange the Na cations and finally calcined at 773 K [12].

Commercially available ZSM-5 with a Si/Al ratio of 40 was supplied by Zeolyst International (CBV8020) in its ammonium form, and was calcined in an air flow at 813 K before its use in reactions.

2.2. Characterization

X-ray powder diffraction (XRD) was recorded using a PANalytical Cubix diffractometer equipped with a graphite monochromator, operating at 40 kV and 45 mA, and utilizing nickel-filtered Cu Kα radiation (λ = 0.1542 nm) to confirm the zeolite structure of the as-synthesized materials and to measure the crystallinity of the catalysts after activation treatments. The chemical composition of the materials was determined using a 715-ES ICP-Optical Emission spectrometer after dissolving the solids in a HNO_3/HF solution. Textural properties were studied through by N_2 adsorption-desorption in a volumetric ASAP 2040 instrument (Micromeritics), with surface area values obtained by applying the BET equation. The morphology of the crystals was studied by scanning electron microscopy (SEM) using a JEOL model JSM 6300 microscope.

The relative concentration of acidic sites in the different samples was obtained by FT-IR spectroscopy using pyridine as the probe molecule. Pyridine adsorption-desorption experiments were carried out on self-supported wafers (10 mg·cm^{-2}) of samples activated at 673 K and 10^{-2} Pa for 2 hours. After wafer activation, the base spectrum was recorded, and pyridine vapor (6.5×10^2 Pa) was introduced into the vacuum IR cell and adsorbed onto the zeolite at 423 K. Desorption was performed in vacuum over three consecutive 1-hour periods of heating at 423, 523, and 623 K, each followed by an IR measurement at room temperature. All spectra were scaled according to sample weight. The numbers of Brønsted and Lewis acid sites were determined from the intensities of the bands at approximately 1545 and 1450 cm^{-1} , respectively, using the molar extinction coefficients provided by Emeis [13]. The external Brønsted acidity was determined using 2,6-di-tert-butylpyridine (DTBPy) following a similar procedure by adsorption on the zeolite at 423 K and desorption in vacuum at this temperature. The concentration of external Brønsted acid sites was determined from the intensities of the bands at approximately 1615 cm^{-1} , using the molar extinction coefficients reported by Góra-Marek et al. [14]

2.3. Catalytic reactivity

The catalytic experiments for the alkylation of benzene or toluene were conducted in the vapor phase, at atmospheric pressure, in a fixed-bed tubular glass reactor (11 mm internal diameter) as previously described [15]. The aromatic/ethanol mixture feed was introduced into the upper part of the reactor by means of a Cole-Palmer syringe pump, nitrogen was used as the carrier gas, maintaining a ratio of aromatic: ethanol:N_2 = 4:1:10. Prior to the addition of reactants, the acid catalyst was heated to 623 K at a rate of 5 K/min under a nitrogen flow. After 30 minutes, the temperature was raised to 723 K and maintained for 1 hour; the reactor was then cooled to the reaction temperature. Experiments were performed under isothermal conditions at 553 K, aiming for similar conversion levels by adjusting the amount of catalyst and the molar flow of reactants. Reaction products were analyzed using a gas chromatograph (Agilent 6890) equipped with a Supelco WAX-10 capillary column (60 m length, 0.2 mm inner diameter) and a flame ionization detector (FID). Results were taken at the very early stages of the reaction (10–360 seconds of time on stream) to detect the effects of catalyst deactivation. Benzene and toluene conversion were normalized according to the molar ratio aromatic = 4:1 in the feed flow. The catalysts were regenerated, in situ, with air flow at 783 K for 5 hours between any experiments.

1,3-Diisopropylbenzene (*m*-DIPB) isomerization and trans-alkylation were conducted in the vapor phase at atmospheric pressure. Nitrogen was used as the carrier gas, with the aromatic compound fed with N_2 flow to achieve a 1:4 molar ratio. The conversion degree was determined from the 1,3-DIPB detected in reactants and products. The activity of the process was evaluated by performing several runs in which the residence time in the catalyst was varied, keeping the mass of the sample loaded (w ≈ 0.1 g) constant while modifying the flow rate of *m*-DIPB fed (F = 0.1–0.6 mL/min).

Conversion was calculated considering F_{k0} initial molar flow of ethanol, benzene, toluene or 1,3-disopropylbenzene (according to feed) and at different time-on-stream (F_k)

$$X(\%) = \frac{F_{k0} - F_k}{F_{k0}} \quad (1)$$

Product selectivity was determined in the aromatic fraction considering de molar flow of each product (F_j) respect to the total, feed free

$$S_j(\%) = \frac{F_j}{\sum_{j=1}^{s} F_j} \quad (2)$$

Deactivation factor values the relative loss of catalyst activity during the time-on-stream considering aromatic initial conversion (X_0) to final conversion at 360 s (X_{360})

$$\textit{Deactivation factor} = \frac{X_0 - X_{360}}{X_0} \quad (3)$$

3. Results and discussion

3.1. Characterization of catalysts

The X-ray diffraction pattern of the ITQ-13 sample confirms the ITH structure of the material [4] [16], as can be seen in Fig. 1a, where the patterns of the three materials are displayed. Scanning Electron Microscopy (SEM) images of ITQ-13 reveal its rod-like morphology and a crystal size in the range of 0.3–0.5 μm (see Fig. 1b). In contrast, the ZSM-5 (CBV8020) exhibits spherical crystallites with sizes around 0.5–0.6 μm [17], and MCM-22, synthesized via the calcination of its laminar MWW precursor, displays thin platelet-like crystals [12]. The physicochemical properties of the materials studied are summarized in Table 1. While the bulk Si/Al ratios are similar among the samples, it is important to note that this comparable aluminum content does not necessarily correlate with similar Brønsted acidity; both framework and extra-framework aluminum species can influence this property. The textural characteristics of ITQ-13 sample align with values reported in the literature [18], with micropore surface area and volume measuring 431 m^2/g and 0.160 cm^3/g, respectively. Notably, the ZSM-5 zeolite exhibits a similar BET surface area, while MCM-22 possesses a greater specific surface area, attributed to the presence of the 12-ring supercage system [12].

Despite ITQ-13 exhibiting a T^4/T^3 ratio similar to that of ZSM-5 (T^4 stands for Si plus Ge and T^3 is Al), its acidity is significantly lower, both

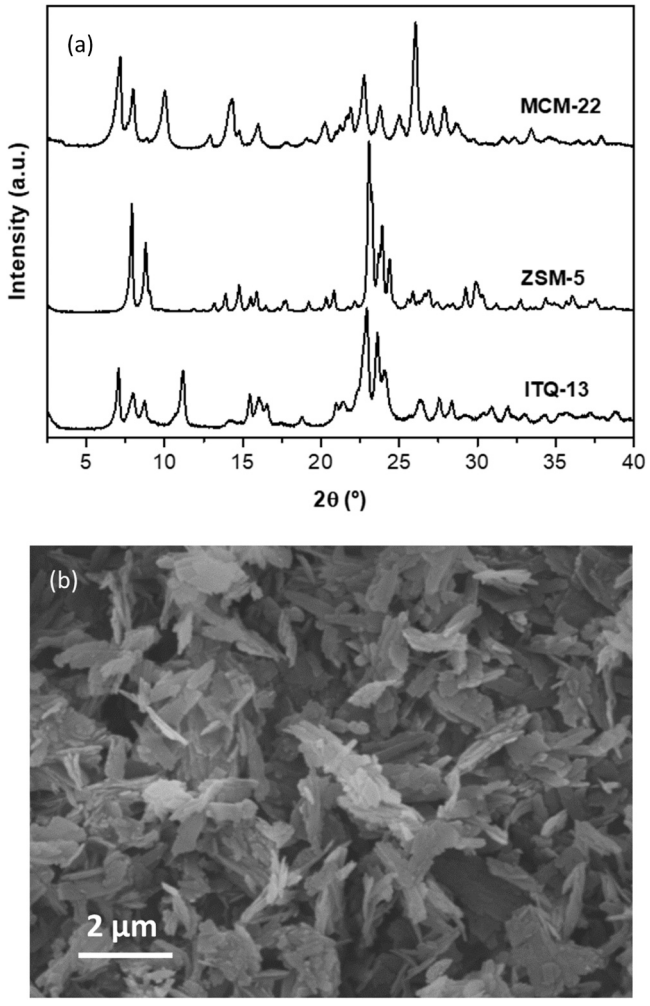

Fig. 1. X-ray diffraction patterns of the zeolites in their acid forms (a); and SEM image of the ITQ-13 zeolite in acid form (b).

Table 1
Characterization of samples used in this work.

Sample	ITQ-13	ZSM-5	MCM-22
T^4/T^{3a} molar ratio	38.7	31.0	50
Si/Ge ratio	13.3	—	—
Crystal size (μm)	0.3–0.5	0.6	0.3
Area BET (m^2/g)	431	433	520
Micropore area (m^2/g)	413	387	475
Micropore volume (cm^3/g)	0.160	0.168	0.185
Brønsted acidity (μmol Py/g)			
423 K	108	222	81
523 K	107	213	74
623 K	66	173	38
Lewis acidity (μmol Py/g)			
423 K	56	22	36
523 K	55	15	31
623 K	46	13	26
External Brønsted acidity (μmol DTBPy/g)			
423 K	39	14	—

[a] T^4 = Si+Ge; T^3 = Al (chemical analysis).

in terms of the total number of Brønsted acid centers and the proportion of the strongest sites capable of retaining pyridine at 623 K. MCM-22 shows slightly lower acidity, as anticipated due to its reduced aluminum content. The results summarized in Table 1 are crucial from a catalytic perspective, as the activity and selectivity of the catalysts are closely related to the total number of Brønsted acid sites (BAS) and their acid strength distribution. This difference may be attributed in ITQ-13 sample to the presence of germanium and to a higher concentration of cationic extraframework aluminum (EFAL) species located in charge-compensating positions, which likely decreases the number of BAS. Indeed, results presented in Table 1 indicate a greater number of Lewis acid sites in ITQ-13. Interestingly, the external acidity determined by using a bulky probe molecule (DTBPy) that is not able to enter within the pores and interacts only with external acid sites shows that the concentration of external Brønsted acid sites in ITQ-13 is almost three times that of ZSM-5. Taking into account the higher total acidity in ZSM-5, this means that the ratio between the number of external versus total acid sites is significantly higher in the case of ITQ-13.

3.2. Alkylation of benzene with ethanol

Zeolites have enabled the development of a sustainable process responsible for 90 % of ethylbenzene production via alkylation [7]. The alkylation of benzene with ethanol can be considered as an electrophilic substitution on the aromatic ring, and over acidic zeolites it is commonly considered as proceeding via a carbenium ion–type mechanism [19]. When alcohol is used as an alkylating agent, the ethylation reaction is proposed to take place by the reaction of the activated alkene (formed by dehydration of the alcohol) on the acid sites of the zeolite. It is generally considered that the activated ethanol is retained on a Brønsted acid center (BAS), and subsequently reacts with the aromatic molecule (benzene or toluene) forming a protonated Wheland complex, which releases hydrogen that is again available in the zeolite [20]. The activated ethanol can react with the aromatic compound, producing monoalkylated or polyalkylated aromatics [21,22]. Additionally, ethanol or ethylene molecules may react to form C4, C6, or C8 olefins, which can subsequently undergo oligomerization, cracking, isomerization, and alkylation reactions, leading to the production of higher oligomers and other alkylaromatics [23], with our equipment we are able to detect significant amounts of cumene, ethyltoluene, *sec*- or *tert*-butylbenzene, and small traces of other larger aromatics in the analysis of the reaction products especially in ZSM-5, which is reflected in Table 2. If these consecutive reactions are excessively favored, coke precursors can form, leading to catalyst deactivation.

Table 2 presents the conversion and selectivity results obtained for benzene alkylation with ethanol using ITQ-13 and the other two

Table 2
Conversion and product distribution in benzene and toluene alkylation with ethanol over ITQ-13, ZSM-5 and MCM-22 samples.

	Benzene Alkylation			Toluene Alkylation		
sample	**ITQ-13**	**ZSM-5**	**MCM22**	**ITQ-13**	**ZSM-5**	**MCM22**
Weight catalysis w_{cat} (mg)	72.1	95.9	120.2	72.1	78.6	105.4
w/F (g·h·mol^{-1})	0.615	0.830	0.520	0.362	1.05	0.707
Aromatic conversion (% mol)	32.3	21.5	37.1	17.1	10.9	13.4
Ethanol conversion (% mol)	74.3	97.7	93.8	63.8	92.5	63.6
Deactivation Factor	38.2 %	51.6 %	41.3 %	17.1 %	74.7 %	42.5 %
Aromatic Selectivity Products (% molar)[a]						
Benzene	–	–	–	0.0	0.0	0.6
Toluene	0.0	0.1	0.5	–	–	–
Ethylbenzene (EB)	87.5	82.0	91.7	0.0	0.6	1.9
Xylenes	0.0	0.1	0.0	0.0	1.0	1.9
Ethyltoluene (ET)	0.0	5.4	0.0	90.5	79.4	91.7
Buthylbenzene	0.0	2.6	0.0	0.0	10.1	1.4
Diethylbenzene (DEB)	12.5	9.6	7.7	0.0	0.0	0.0
Diethyltoluene (DET)	0.0	0.0	0.0	9.5	2.1	2.0
Others	0.0	0.3	0.1	0.0	6.8	0.6
Ethanol Product distribution (% molar)						
Olefins & Oligomers	15.7	52.6	33.7	18.9	60.5	26.1
Aromatics	58.6	45.1	60.1	44.9	31.9	37.4
Rest in products	25.7	2.3	6.2	36.2	7.5	36.4
Aromatic/Ethylene ratio	21.3	4.0	7.3	2.4	0.52	1.4

Note: reaction conditions: Aromatic:Ethanol:N_2 ratio = 4:1:10, T = 553 K, conversion at 10 s TOS.
[a] Benzene or Toluene free.

medium-pore zeolites, MCM-22 and ZSM-5. The data indicate that the primary product in all cases is ethylbenzene, followed by diethylbenzenes, while toluene, buthylbenzenes, and other aromatics are present in significantly smaller quantities.

Fig. 2 illustrates the normalized conversion of benzene and ethanol achieved at short times on stream (TOS = 10 s), conditions under which catalyst deactivation effects are minimized, as a function of the contact time (w/F). The results demonstrate that both ITQ-13 and MCM-22 give higher benzene conversion than ZSM-5, despite their lower Brønsted acidity. However, ITQ-13 is the least active in terms of ethanol conversion.

Concerning EB selectivity ITQ-13 outperforms ZSM-5 (Table 2) and gives comparable values to those obtained with MCM-22, which is commercially utilized for this process [8]. Notably, ITQ-13 zeolite produces only diethylbenzene (DEB) as by-product, which could be used for other applications or transformed into more ethylbenzene in a subsequent transalkylation unit by reaction with benzene [24]. The product distribution obtained with MCM-22 is similar, exhibiting selectivity values for EB and DEB aromatic products close to 100 %, with minimal contributions of olefin oligomerization reactions. These undesired parallel reactions contribute to catalyst deactivation and diminish the selectivity to EB in the aromatic fraction by forming olefins other than ethylene, which can further alkylate aromatic molecules [25]. In the case of ZSM-5 significant amounts of ethyltoluene and butylbenzenes have been detected in the outlet stream products not observed in ITQ-13 or MCM-22.

If we consider the distribution of the products obtained from ethanol (Table 2), it can be observed that in ZSM-5 a significant part of the ethanol reacts to give ethylene or other compounds developed from the oligomerization process, and to a lesser extent it reacts with aromatic molecules. In the case of zeolite ITQ-13 the evolution is exactly the opposite, that is, most of the ethanol reacts to form primary aromatic products (EB) or secondary (DEB). Zeolite MCM-22 shows an intermediate distribution with respect to those mentioned above, also giving a

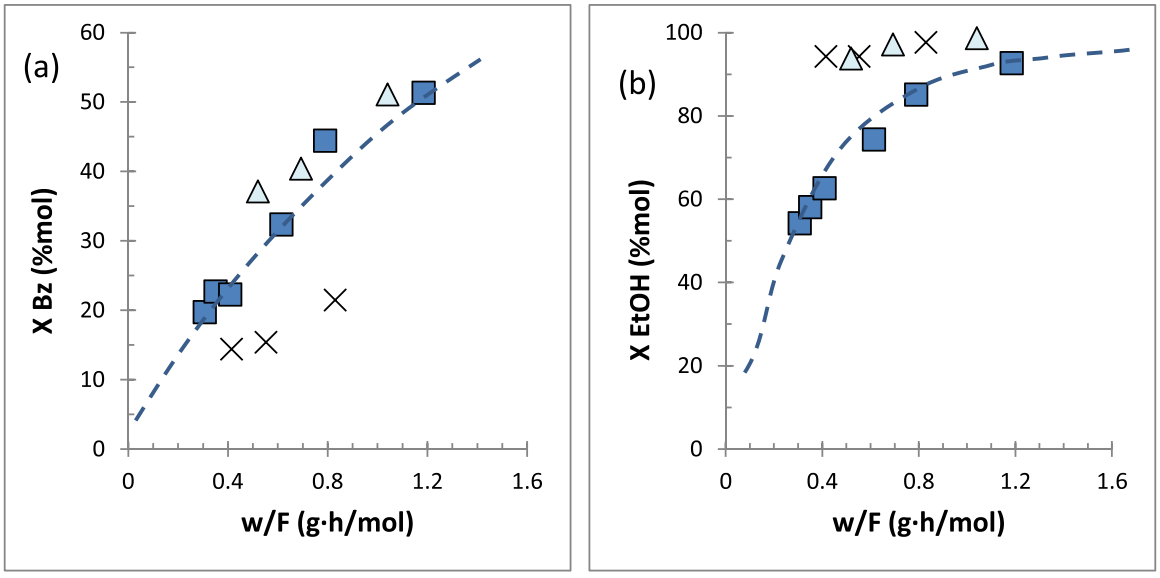

Fig. 2. Normalized conversion (X) of: (a) Benzene (Bz), (b) Ethanol (EtOH) versus contact time (w/F). Catalysts: ITQ-13 (■), MCM-22 (Δ), ZSM-5 (×) (553 K, Bz: EtOH:N_2 molar ratio = 4:1:10).

good proportion of alkylation products. This ultimately extends the lifespan of these catalysts, as illustrated by their lower deactivation factors (Table 2). Furthermore, the lower ethanol conversion capacity of ITQ-13 results in a higher aromatic/ethylene ratio compared to ZSM-5 and MCM-22 (Table 2), where ethanol conversion is higher. This could be a possible explanation for its high EB selectivity and longer catalyst life.

3.3. Alkylation of toluene with ethanol

The alkylation of toluene with ethanol yields ethyltoluenes (ET), with *para*-ET being the isomer of greatest industrial interest. Medium-pore zeolites serve as effective and selective catalysts for this process [21,26]. Fig. 3 show the normalized conversion of toluene and ethanol as a function of contact time (w/F). Notably, ITQ-13 achieves high activity for the conversion of both reagents, surpassing both MCM-22 and ZSM-5 for toluene conversion, despite having lower Brønsted acidity. It is important to note that zeolitic structures exhibiting higher activity typically contain cavities where the formation of additional reaction products may be favored [27].

Table 2 presents the product selectivity across the different catalysts at comparable conversion levels. In all cases, the primary product are ethyltoluenes (ET). ITQ-13 exhibits the high selectivity for the mono-alkylation product, with values above 90 %, regardless of toluene conversion, and surpassing the obtained with ZSM-5. Experimental evidence indicates that the selectivity for ET with various ZSM-5 samples is independent of the density of acid centers or crystal size [28], suggesting that zeolite topology significantly plays a major role in terms of product distribution.

The alkylation process can also lead to the formation of diethyltoluenes (DET) (see Table 2). which are valuable products that can be converted into additional ethyltoluene through transalkylation reactions with toluene [24]. Among the zeolites studied, ITQ-13 is the most selective, giving only alkylation products, reaching values of the sum of ET and DET close to 100 %. If we consider again the distribution of ethanol (Table 2), it can be observed that in ZSM-5 a significant part of the ethanol reacts to give ethylene or other oligomerization compounds, and to a lesser extent it reacts with toluene. In the case of zeolite ITQ-13 the evolution is exactly the opposite, i.e. most of the ethanol reacts to form primary aromatic products (ET) or secondary (DET). Zeolite MCM-22 shows an intermediate distribution with respect to those mentioned above, also giving a good proportion of alkylation products. In addition, small amounts of ethylbenzene and xylenes are detected in ZSM-5 and MCM-22, which could be related to the possibility of toluene disproportionation, which requires sufficient space to form diphenyl-type reaction intermediates, something that is not observed in ITQ-13. A lower deactivation factor is also observed again in the ITQ-13 sample.

Based on the product distribution presented in Table 2, ITQ-13 emerges as the most suitable zeolite for the production of ethylbenzene (EB) and ethyltoluene (ET). This high selectivity to the mono- and di-alkylated products is maintained along the whole conversion range studied for both processes, alkylation of benzene and toluene, with values reaching levels close to 100 %, as can be seen in Fig. 4.

The formation of these byproducts can significantly impact the feasibility of the catalyst for industrial applications, as it reduces process efficiency and increases the cost of subsequent separation processes. Therefore, achieving high yields of the main product is crucial.

3.4. Dialkyl-isomer distribution

Fig. 5 displays the normalized distribution of diethylbenzene and ethyltoluene isomers obtained with the studied zeolite for benzene dialkylation (a) and toluene alkylation (b) with ethanol, respectively. It should be noted that ethyltoluenes are primary reaction products between toluene and ethanol, while diethylbenzenes are produced in a secondary alkylation of ethylbenzene produced with ethanol, which partly conditions the distribution of these isomers in the channels of medium pore zeolites, where the relative sizes of larger isomers are more limited in their conformation and diffusion.

In the case of the 9-MR channel in ITQ-13, previous studies have shown that the diffusion of *para*-xylene [15] is possible, but it is much more restricted than in the 10-MR channel, while *ortho*-xylene or *meta*-xylene, do not even enter the 9 MR due to severe size restrictions, and consequently this smaller channel system is of little use for diffusing xylenes or other larger aromatics. Although in ITQ-13 and ZSM-5 diffusion occurs through 10-MR pores, in ITQ-13 it should additionally be noted that these channels are connected through the larger 15.5 Å void space. The presence of these larger void spaces will negatively influence diffusion. Indeed, when the molecule diffuses through the 10-MR channel in ITQ-13 and is diverted into the large cavity, this acts as a diffusion trap in which the molecule experiences extensive local

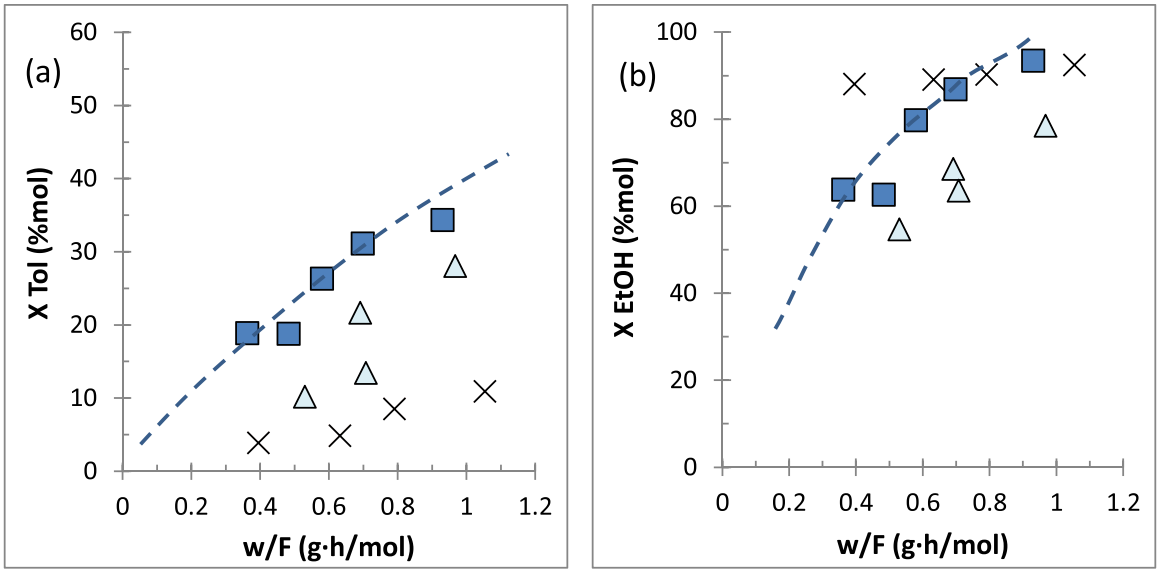

Fig. 3. Normalized conversion (X) of: (a) Toluene (Tol), (b) Ethanol (EtOH) versus contact time (w/F). Catalysts: ITQ-13 (■), MCM-22 (Δ), ZSM-5 (×) (553 K, Tol: EtOH:N_2 molar ratio = 4:1:10).

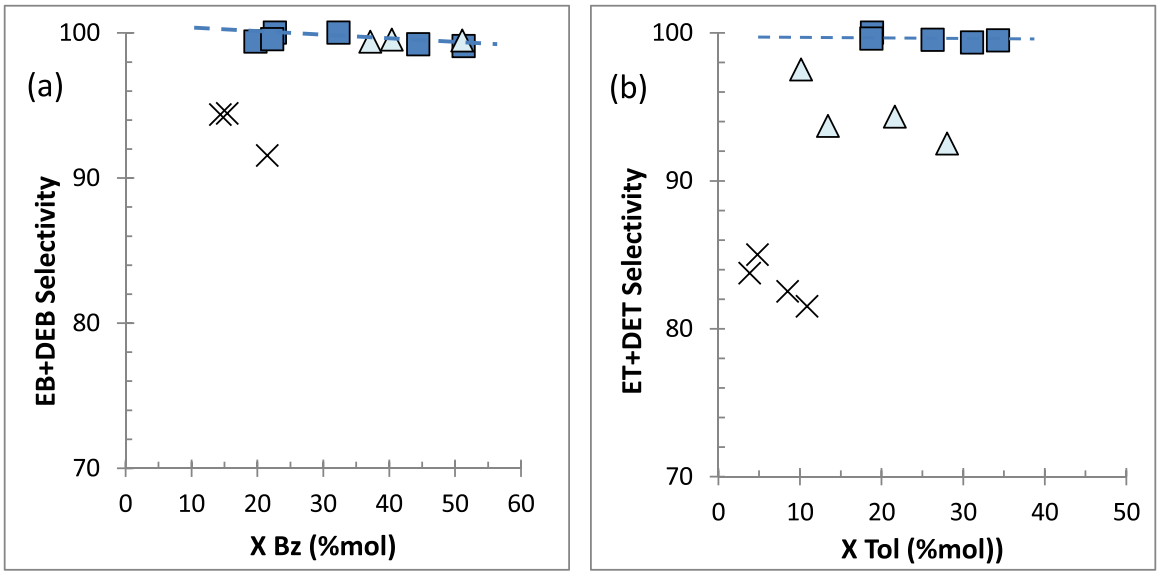

Fig. 4. Aromatic selectivity of (a) EB+DEB versus benzene conversion (X Bz), (b) ET+DET versus toluene conversion (X Tol). Catalysts: ITQ-13 (■), MCM-22 (Δ), ZSM-5 (×) (553 K, Aromatic:EtOH:N_2 molar ratio = 4:1:10).

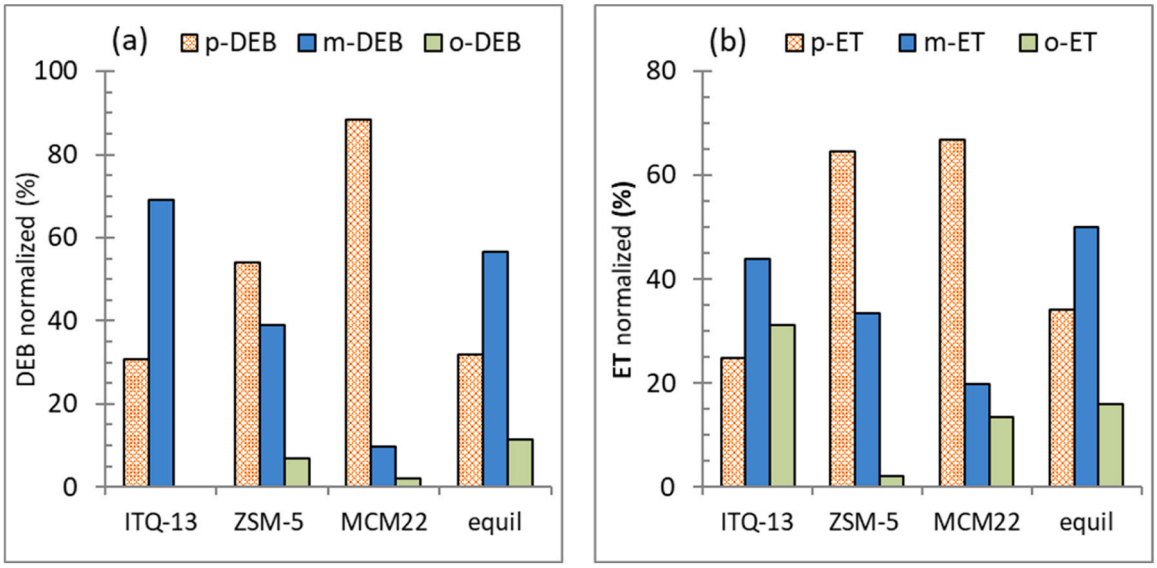

Fig. 5. (a) Diethylbenzene (DEB) and (b) Ethyltoluene (ET) normalized isomer distribution in benzene (a) or toluene (b) alkylation with ethanol at 553 K. (Aromatic: Ethanol:N_2 molar ratio = 4:1:10).

motion that slows its progress.

In both cases ITQ-13 shows a dialkyl-aromatic product distribution close to that corresponding to the equilibrium at the reaction temperature, exhibiting a completely different behavior as compared to ZSM-5 or MCM-22, which favor *para*-selectivity during alkylation with ethanol (see Fig. 5 and Table 2). However, in the case of DEB, with a larger molecular size as compared to ET, the *ortho*-isomer is not observed, deviating the distribution from the thermodynamically favored. This phenomenon may be attributed to the ease of forming different products and their diffusion within the cavities and channels. As the products become bulkier (such as in dialkylation with ethanol), the steric hindrance may impede the diffusion of the larger *ortho*-isomers. Unexpectedly, the predominant isomer obtained in both alkylation processes with ITQ-13 is the *meta* isomer, which, according to the commonly proposed mechanism for an electrophilic substitution, is formed through an isomerization process of the *para* or *ortho* isomers generated as primary toluene or ethylbenzene alkylation products.

Fig. 5a compares the distribution of DEB isomers, which varies significantly between zeolites. The *ortho* isomer is the least abundant in the three cases, practically not detected in ITQ-13, which is determined by its larger size, which will condition the difficulties in its formation and diffusion through the 10-MR channels. The predominant isomer produced by ITQ-13 is *m*-DEB, which is more favored thermodynamically. The ratio of *p*-/*m*-DEB is similar to that obtained at thermodynamic equilibrium, possibly due to the increased residence time of DEBs within the cavities. *m*-DEB isomers can diffuse through the channels parallel to the *b*- and *c*-axes, as confirmed by theoretical studies [15]. Additionally, contributions from the structured external surface and its lower acidity cannot be discarded. In contrast, the main isomer for ZSM-5 and MCM-22 is *p*-DEB, with MCM-22 exhibiting significantly greater *para*-selectivity, likely due to the more stringent constraints of its smaller 10-ring circular channels. Although traditionally *p*-DEB has been the most demanded isomer, *m*-DEB has been recently highlighted as an important intermediary for obtaining various fine chemicals [29].

Within the ethyltoluene fraction, selectivity also varies considerably among the structures compared. As for DEB, the *p*-isomer predominates in the case of ZSM-5 and MCM-22, (with selectivity above 50 % within the ET fraction), although the *p/o* ratio is much higher for ZSM-5 (Fig. 5b). In contrast, ITQ-13 presents a unique distribution, with a higher proportion of *o*-ET as compared to *p*-ET (*p/o* ratio less than 1). This catalytic behavior may be influenced by different factors, such as the longer residence times of the alkylation products within the cavities defined by its channel system, its lower acidity and the enhanced activity of its external surface [6]. Furthermore, according to the electrophilic substitution of toluene, it should be noted that there would be two ethylation positions leading to the *o*-ET, while only one position would lead to the *p*- ET. The evolution towards the *m*-ET isomer would be determined by isomerization influenced by the availability of centers and space in the channels and cavities. On the other hand, MCM-22 exhibits greater selectivity towards benzene, ethylbenzene, and xylenes than ITQ-13, which underscores a more significant extent of toluene disproportionation reactions occurring within its cavities [15].

3.5. Catalyst deactivation

In the alkylation of benzene or toluene with ethanol, the catalysts undergo a deactivation process as the reaction progresses, primarily due to the formation of bulky products within the channels and cavities and/or their intersections, which can obstruct the zeolite's pores. As shown in Table 2, ITQ-13 exhibits the smallest deactivation factors in both alkylation processes, indicating that it experiences the slowest loss of activity over the studied reaction time.

Catalytic deactivation has been assessed by monitoring the conversion as a function of time on stream (TOS) during the benzene and toluene alkylation processes (see Fig. 6). Conversion decreases with TOS regardless of the catalyst used; however, deactivation rate is lower with ITQ-13 as compared to MCM-22 and ZSM-5. This observation may be related to the stability and diffusion of the formed products within the zeolite channel structures [30]. In the case of ZSM-5, ethanol oligomerization can lead to coke formation in relatively short timeframes. For MCM-22, the formation of certain products may occur at the "cups" on the external surface, resulting in lower deactivation compared to ZSM-5. The deactivation effects are similar for both toluene and benzene, as illustrated in Fig. 6 for alkylation with ethanol. The curve plotted corresponds to an exponential function, as is usually in this type of process.

$$\frac{X(t)}{X_0} = \exp(-k_d \cdot t^{0.5}) \quad (4)$$

From an industrial perspective, this consistency in performance could be advantageous, as it would stabilize the reactor exit composition, thereby extending the useful life of the catalyst.

Throughout this study we have discussed on the possibility that the external or more easily accessible surface of the catalysts could partly condition the product distribution achieved. For this reason, we have considered examining the behavior of zeolites ZSM-5 and ITQ-13 in the reactive processing of a larger molecule, 1,3-diisopropylbenzene (1,3-DIPB), which cannot diffuse through the 10MR channels. Consequently, only the active sites located on the external surface or near the channel openings are likely responsible for the transformations involved. The results obtained in this process are summarized in Fig. 7.

The conversion achieved under the same experimental conditions is significantly higher for ITQ-13 than for ZSM-5. This confirms what was already pointed out with the 2,6-DTBPy adsorption tests, which

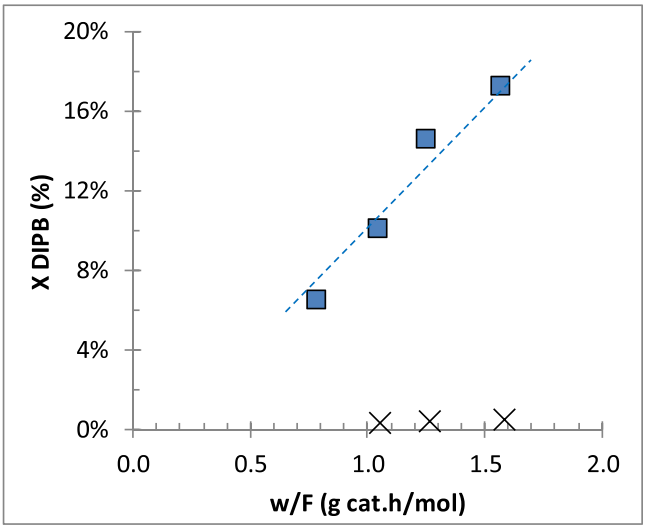

Fig. 7. Conversion of: 1,3-DIPB (X) versus contact time (w/F). Catalysts: ITQ-13 (■), ZSM-5 (×) (553 K, 1,3-DIPB:N_2 molar ratio = 1:4, 10 s time-on-stream).

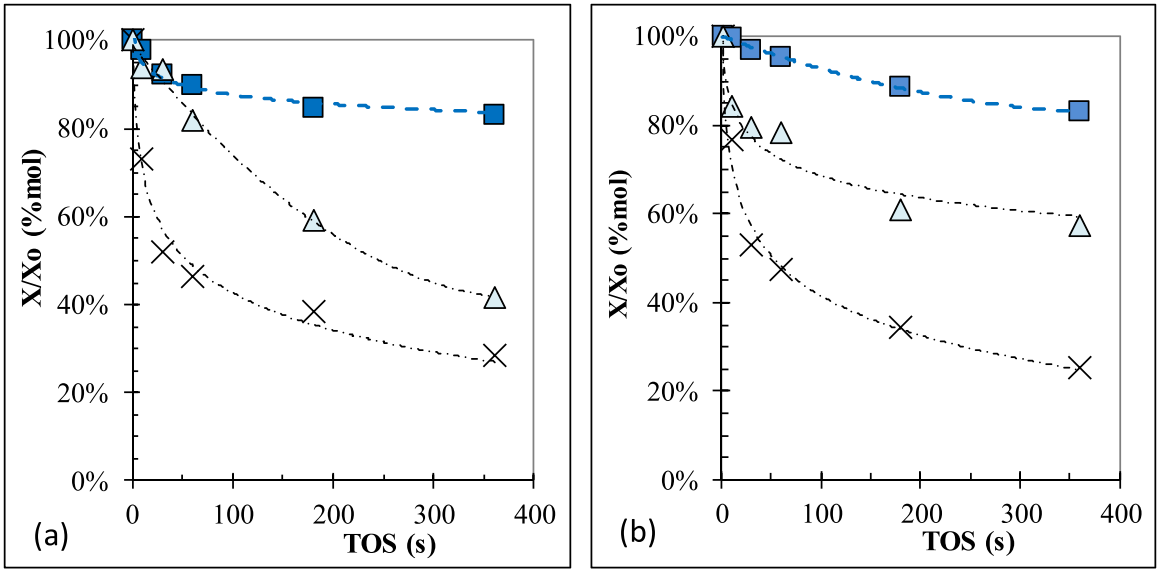

Fig. 6. Deactivation effect benzene (a) or toluene (b) alkylation with ethanol (X/Xo) at 553 K versus time-on-stream (TOS). Catalysts: ITQ-13 (■), MCM-22 (Δ), ZSM-5 (×) (Aromatic:Ethanol:N_2 molar ratio = 4:1:10).

indicated that the amount of accessible active sites available for the conversion of this bulky molecule (1,3-DIPB) is considerably higher in ITQ-13 compared to ZSM-5. The main products generated are light olefins (propylene and butenes), produced through dealkylation processes, beside aromatic products such as cumene, 1,4-DIPB, and 1,3,5-triisopropylbenzene (1,3,5-TIPB).

These results should be taken into consideration to justify, at least in part, the high activity of ITQ-13, the distribution of isomers to *mono*- and *di*-ethylated products, the close-to-thermodynamic distribution and its lower deactivation by pore blocking, already indicated, corroborating the hypotheses formulated regarding the possible influence of easily accessible active centers in this zeolite. In the case of ZSM-5 and MCM-22, the dominance of reactions within the pores relative to the external surface leads to isomer screening behavior favoring *para* products

4. Conclusions

Zeolite ITQ-13 demonstrates high catalytic activity and selectivity for the production of ethylbenzene and ethyltoluenes, outperforming ZSM-5 and showing comparable performance to MCM-22, despite its lower Brønsted acidity. Notably, ITQ-13 presents longer catalyst life, with byproducts primarily consisting of dialkylated compounds that could be utilized in subsequent processes.

Unexpectedly, the predominant isomer obtained in both alkylation processes with ITQ-13 is the *meta* isomer, which, according to the commonly proposed mechanism for an electrophilic substitution, is formed through an isomerization process of the *para* or *ortho* isomers generated as primary toluene or ethylbenzene alkylation products. Throughout this study we have discussed the possible contribution of the particular channels system of ITQ-13, with cavities at the channel intersections, or of the external or more easily accessible surface active sites, which could partly condition the product distribution achieved.

The use of ITQ-13 zeolite in the alkylation of aromatic compounds with ethanol offers several advantages in terms of sustainability, enhanced reaction efficiency, leading to higher yields of alkylated aromatics while minimizing by-products and waste.

CRediT authorship contribution statement

Llopis Francisco J.: Supervision, Methodology, Investigation. **Portilla M. Teresa:** Validation, Methodology, Investigation, Formal analysis. **Corma Avelino:** Writing – review & editing, Supervision, Conceptualization. **Martínez Cristina:** Writing – review & editing, Validation, Supervision, Resources, Funding acquisition, Formal analysis. **Valencia Susana:** Writing – review & editing, Validation, Supervision, Resources, Formal analysis.

Declaration of Competing Interest

The authors declare that they have no known competing financial interests or personal relationships that could have appeared to influence the work reported in this paper.

Acknowledgements

Financial support by the Spanish Ministry of Science and Innovation is gratefully acknowledged (CEX2021–001230-S, PID2021-1227550B-I00 and PID2022-136934OB-100 grants funded by MCIN/AEI/10.13039/501100011033; and TED2021-130191B-C41 grant funded by the European Union NextGenerationEU/PRTR). The authors thank also the financial support of the Generalitat Valenciana through the Prometeo Program (CIPROM/2023/34 and Prometeo 2021/077). Finally, the authors acknowledge the Electron Microscopy Service of the Universitat Politècnica de València (UPV) for assistance in electron microscopy characterization.

Data availability

Data will be made available on request.

References

[1] A. Corma, State of the art and future challenges of zeolites as catalysts, J. Catal. 216 (2003) 298–312, https://doi.org/10.1016/S0021-9517(02)00132-X.
[2] C.S. Cundy, P.A. Cox, The hydrothermal synthesis of zeolites: history and development from the earliest days to the present time, Chem. Rev. 103 (2003) 663–702, https://doi.org/10.1021/cr020060i.
[3] C. Baerlocher, L.B. McCusker, D.H. Olson, Atlas of Zeolite Framework Types, Elsevier, 2007.
[4] A. Corma, M. Puche, F. Rey, G. Sankar, A zeolite structure (ITQ-13) with three sets of medium-pore crossing channels formed by 9- and 10-Rings, Angewandle Chem. 115 (2003) 1188–1191, https://doi.org/10.1002/ange.200390275.
[5] C. Martínez, A. Corma, Inorganic molecular sieves: preparation, modification and industrial application in catalytic processes, Coord. Chem. Rev. 255 (2011) 1558–1580, https://doi.org/10.1016/j.ccr.2011.03.014.
[6] Y. Li, L. Li, J. Yu, Applications of zeolites in sustainable chemistry, Chem 3 (2017) 928–949, https://doi.org/10.1016/j.chempr.2017.10.009.
[7] K. Tanabe, W.F. Hölderich, Industrial application of solid acid–base catalysts, Appl. Catal. A Gen. 181 (1999) 399–434, https://doi.org/10.1016/S0926-860X(98)00397-4.
[8] N.Y. Chen, Industrial application of shape selective catalysis, Stud. Surf. Sci. Catal. 38 (1988) 153–163, https://doi.org/10.1016/S0167-2991(09)60652-2.
[9] R. Castañeda, A. Corma, V. Fornés, J. Martínez-Triguero, S. Valencia, Direct synthesis of a 9 × 10 member ring zeolite (Al-ITQ-13): a highly shape-selective catalyst for catalytic cracking, J. Catal. 238 (2006) 79–87, https://doi.org/10.1016/j.jcat.2005.11.038.
[10] UPV, Standard procedure for working with hydrofluoric acid, 2010. ⟨https://www.sprl.upv.es/D7_2_12_b.htm⟩.
[11] M.E. Leonowicz, J.A. Lawton, S.L. Lawton, M.K. Rubin, MCM-22: a molecular sieve with two independent multidimensional channel systems, Science 264 (1994) 1910–1913, https://doi.org/10.1126/SCIENCE.264.5167.1910.
[12] A. Corma, C. Corell, J. Pérez-Pariente, Synthesis and characterization of the MCM-22 zeolite, Zeolites 15 (1995) 2–8, https://doi.org/10.1016/0144-2449(94)00013-I.
[13] C.A. Emeis, Determination of integrated molar extinction coefficients for infrared absorption bands of pyridine adsorbed on solid acid catalysts, J. Catal. 141 (1993) 347–354, https://doi.org/10.1006/JCAT.1993.1145.
[14] K. Góra-Marek, K. Tarach, M. Choi, 2,6-Di-tert-butylpyridine sorption approach to quantify the external acidity in hierarchical zeolites, J. Phys. Chem. C. 118 (2014) 12266–12274, https://doi.org/10.1021/jp501928k.
[15] F.J. Llopis, G. Sastre, A. Corma, Isomerization and disproportionation of m-xylene in a zeolite with 9- and 10-membered ring pores: molecular dynamics and catalytic studies, J. Catal. 242 (2006) 195–206, https://doi.org/10.1016/j.jcat.2006.05.034.
[16] A. Corma, F. Rey, V. Fornés, R. Castañeda, WO 2005/040041 A1, (2005).
[17] A. Corma, C. Martínez, E. Doskocil, Designing MFI-based catalysts with improved catalyst life for $C3^{=}$ and $C5^{=}$ oligomerization to high-quality liquid fuels, J. Catal. 300 (2013) 183–196, https://doi.org/10.1016/J.JCAT.2012.12.029.
[18] G.G. Juttu, R.F. Lobo, Characterization and catalytic properties of MCM-56 and MCM-22 zeolites, Microporous Mesoporous Mater. 40 (2000) 9–23, https://doi.org/10.1016/S1387-1811(00)00233-X.
[19] S. Siffert, L. Gaillard, B.L. Su, Alkylation of benzene by propene on a series of Beta zeolites: toward a better understanding of the mechanisms, J. Mol. Catal. A Chem. 153 (2000) 267–279, https://doi.org/10.1016/S1381-1169(99)00357-X.
[20] M. Bocus, L. Vanduyfhuys, F. De Proft, B.M. Weckhuysen, V. Van Speybroeck, Mechanistic characterization of zeolite-catalyzed aromatic electrophilic substitution at realistic operating conditions 2 (2022) 502–514, https://doi.org/10.1021/jacsau.1c00544.
[21] J. Čejka, B. Wichterlová, Acid-catalyzed synthesis of mono- and dialkyl benzenes over zeolites: active sites, zeolite topology, and reaction mechanisms, Catal. Rev. 44 (2002) 375–421, https://doi.org/10.1081/CR-120005741.
[22] Y. Du, H. Wang, S. Chen, Study on alkylation of benzene with ethylene over β-zeolite catalyst to ethylbenzene by in situ IR, J. Mol. Catal. A Chem. 179 (2002) 253–261, https://doi.org/10.1016/S1381-1169(01)00384-3.
[23] K.K. Ramasamy, Y. Wang, Catalyst activity comparison of alcohols over zeolites, J. Energy Chem. 22 (2013) 65–71, https://doi.org/10.1016/S2095-4956(13)60008-X.
[24] L. Forni, G. Cremona, F. Missineo, G. Bellussi, C. Perego, G. Pazzuconi, Transalkylation of m-diethylbenzene over large-pore zeolites, Appl. Catal. A Gen. 121 (1995) 261–272, https://doi.org/10.1016/0926-860X(94)00209-6.
[25] L. Pinard, S. Hamieh, C. Canaff, F. Ferreira Madeira, I. Batonneau-Gener, S. Maury, O. Delpoux, K. Ben Tayeb, Y. Pouilloux, H. Vezin, Growth mechanism of coke on HBEA zeolite during ethanol transformation, J. Catal. 299 (2013) 284–297, https://doi.org/10.1016/J.JCAT.2012.12.018.
[26] C. Perego, P. Pollesel, Advances in aromatics processing using zeolite catalysts, Adv. Nanoporous Mater. 1 (2010) 97–149, https://doi.org/10.1016/S1878-7959(09)00102-9.
[27] W. Zhang, S. Lin, Y. Wei, P. Tian, M. Ye, Z. Liu, Cavity-controlled methanol conversion over zeolite catalysts, Natl. Sci. Rev. 10 (2023) nwad120, https://doi.org/10.1093/nsr/nwad120.

[28] M.T. Portilla, "Zeolites for obtaining and redistributing aromatics in the BTX fraction" Thesis Doctoral UPV, Valencia (Spain), (2015), https://doi.org/10.4995/Thesis/10251/59471.
[29] S. Wang, J. Li, Q. Xu, S. Song, Y. Jiang, L. Chen, X. Shi, W. Cheng, Synthesis of spherical nano-ZSM-5 zeolite with intergranular mesoporous for alkylation of ethylbenzene with ethanol to produce m-diethylbenzene, Chin. J. Chem. Eng. 67 (2024) 298–309, https://doi.org/10.1016/J.CJCHE.2023.11.015.
[30] G. Sastre, A. Corma, The confinement effect in zeolites, J. Mol. Catal. A Chem. 305 (2009) 3–7, https://doi.org/10.1016/J.MOLCATA.2008.10.042.